Low Enriched UO_2 Pin Lattice in Water Critical Benchmark Evaluations Using MCNPX with ENDF/B-VII Nuclear Data

John F. Zino*[1], Vernon W. Mills[1] and David D. Dixon[2]
[1]*Global Nuclear Fuel – Americas, 3901 Castle Hayne Road, Wilmington, NC 28402*
[2]*North Carolina State University, Dept. of Nuclear Engineering, Raleigh, NC, 27695*

Abstract

This paper provides benchmark comparisons of the MCNPX Monte Carlo code to a series of integral critical experiments performed at the Toshiba Nuclear Critical Assembly (NCA) facility from 1994 to 2001 [1;2]. The beta-1 release version of ENDF/B-VII is used for all nuclides process with NJOY99 (update 96) executed with the beta test version of MCNPX 2.6.A [3]. A total of fifty-two (52) low enriched, UO_2 pin-lattice in water experiments were analyzed with experimental W/F ratios from 0.791 to 1.756. The lattices were designed to simulate that of 8x8 and 9x9 Boiling Water Reactor (BWR) lattices with hollow aluminum tubes inserted between the fuel rods to simulate voiding conditions in approximately half of the experiments. In addition to measured critical lattice configurations, a series of individual pin-power fission density estimates were made via gross gamma scans of individual fuel pins after irradiation. This data is also used to benchmark the Monte Carlo fission density calculations to confirm the code and cross-section applicability for use as a benchmarking tool for the LANCER02 lattice physics code [4].

KEYWORDS: Critical Benchmarks, NCA Facility, Monte Carlo, Fission Density

1 Introduction

From 1994 to 2001, a series of integral critical test experiments were performed for 8x8 and 9x9 fuel lattices at the Toshiba NCA facility. The NCA facility is an open-vessel tank critical system whereby low-enriched UO_2 pin lattices can be constructed. Figure 1 shows a schematic of the facility [1;2]. Unirradiated UO_2 and UO_2/Gad fuel pins are held at a fixed lattice pitch by upper and lower grid spacer plates attached to the lower fuel support plate and tank respectively. The small-core arrangement essentially consists of a 2x2 array of interior fuel bundle/lattices (test zone) surrounded by an array of UO_2 pins that simulate up to twelve (driver zone) bundle/lattices (Figure 2). The test zone bundle/lattices contain different combinations 3%, 4% and 5% enriched UO_2 pins with several UO_2-Gad(5%) burnable absorber pins. In addition, the test zone can also contain hollow (voided) aluminum tubes that are inserted between the fuel pins

* Corresponding author, Tel. 910-675-6116, Fax. 910-675-6614, E-mail: John.Zino@gnf.com

to simulate the effects of voiding within the lattice. The driver zone fuel pins are 2% enriched UO_2 rods and can be arranged around the test zone bundle/lattices as needed to increase the system reactivity to obtain a critical configuration in combination with adjusting the water level height within the tank.

Figure 1: Schematic of NCA Test Facility.

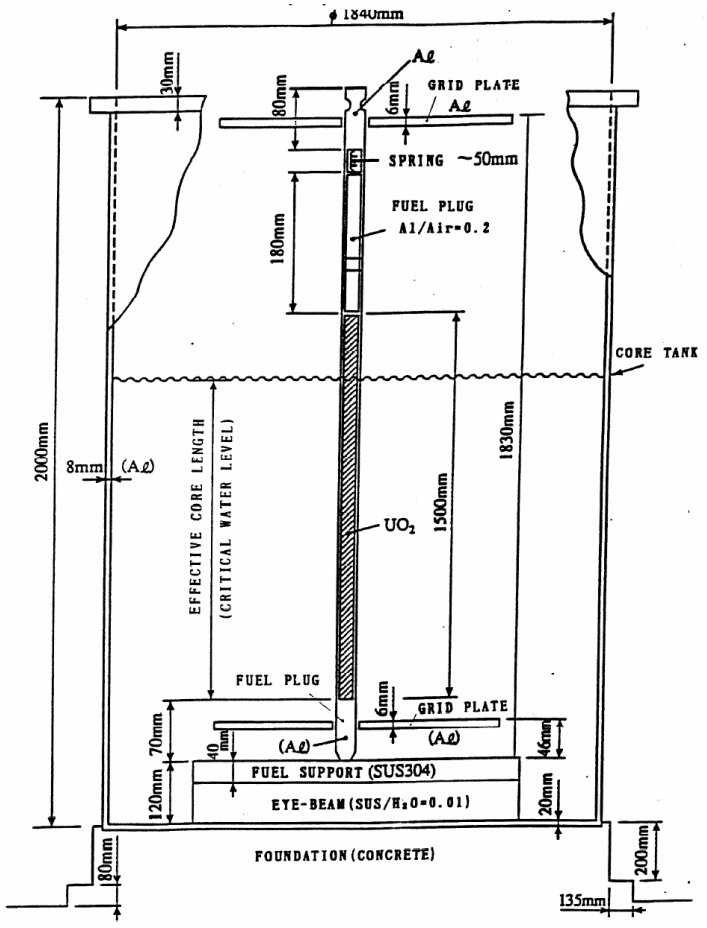

2 Eigenvalue Benchmark Comparisons

Table 1 shows the MCNPX calculated combined collision/absorption/track length eigenvalue estimations for each of the fifty-two observed critical experimental conditions for simulated cold 0% void, hot 0% void and hot 40% void fraction conditions. Also shown in the Table 1 are the number of 5% wt. Gad rods in the test zone, the number of empty (water) rods in the test zone and the average critical water level height in the tank during the test. For cases that have the same number of Gad and water rods, the placement of the rods in the test zone lattice was varied. Since almost all experiments were performed twice for repeatability, the average of the two observed critical water height dimensions is reported for each experiment. The largest difference in observed critical water heights for any one experiment was less than 0.5 cm.

Figure 2: NCA Lattice with Void Tubes in Test Zone.

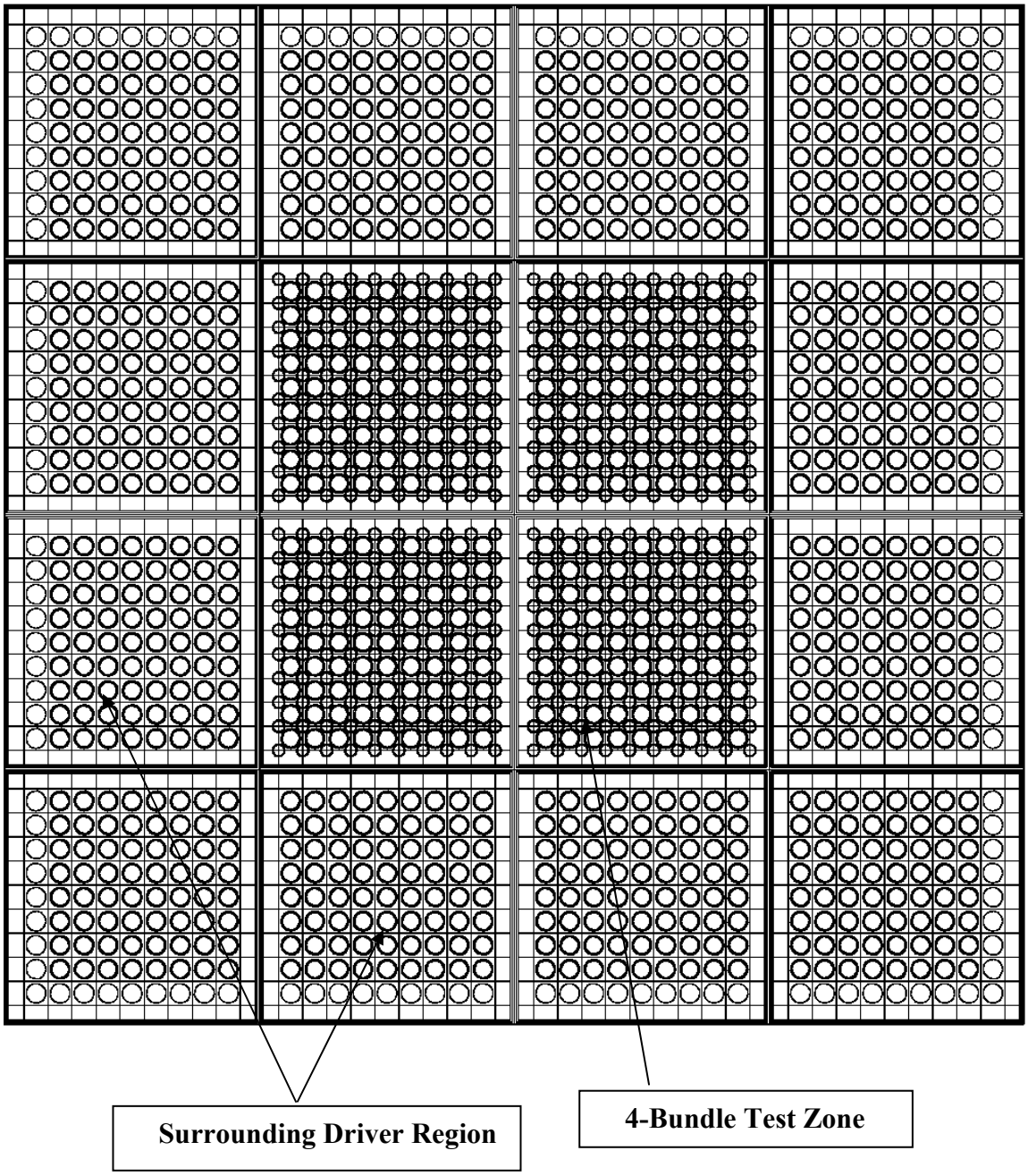

Table 1: NCA Critical Benchmark Results Using ENDF/B-VII Data.

Case ID	# Gd Rods	# Water Rods	Test Zone (W/F)	Avg. Critical Water Height (cm)	MCNPX Results
1	16	13	1.014	118.02	1.00043±0.00014
2	16	7	0.824	103.63	1.00003±0.00015
3	8	13	1.014	87.40	0.99910±0.00014
4	8	13	1.014	118.86	1.00019±0.00014
5	8	7	0.824	79.66	0.99951±0.00014
6	8	7	0.824	101.43	0.99964±0.00014
7	8	13	1.014	86.29	0.99910±0.00015
8	8	13	1.014	116.02	1.00009±0.00014
9	4	13	1.014	77.01	0.99873±0.00014
10	4	13	1.014	97.36	0.99947±0.00015
11	4	7	0.824	78.77	0.99883±0.00016
12	16	13	1.014	137.89	0.99964±0.00015
13	8	13	1.014	83.56	0.99922±0.00014
14	8	13	1.014	109.57	1.00001±0.00015
15	8	7	0.824	82.57	0.99909±0.00014
16	8	7	0.824	107.63	0.99997±0.00014
17	12	13	1.014	93.85	1.00073±0.00013
18	12	13	1.014	136.75	1.00104±0.00013
19	12	7	0.824	86.89	1.00002±0.00014
20	12	7	0.824	118.24	1.00015±0.00014
21	16	13	1.676	99.44	0.99975±0.00013
22	16	7	1.431	80.69	0.99920±0.00014
23	16	7	1.431	104.25	0.99920±0.00014
24	8	13	1.676	87.54	0.99895±0.00014
25	8	13	1.676	123.34	0.99904±0.00015
26	8	7	1.431	84.78	0.99934±0.00014
27	8	7	1.431	121.57	0.99936±0.00015
28	8	13	1.676	108.51	0.99921±0.00015
29	4	13	1.676	75.59	0.99948±0.00014
30	4	13	1.676	104.35	0.99996±0.00015
31	4	7	1.431	92.68	1.00009±0.00016
32	16	13	1.676	120.25	0.99947±0.00013
33	4	13	1.676	74.76	0.99967±0.00015
34	8	13	1.676	98.47	0.99947±0.00014
35	8	7	1.431	84.94	0.99935±0.00015
36	12	13	1.676	95.32	1.00082±0.00014
37	12	7	1.431	78.38	1.00067±0.00014
38	8	7	1.756	96.92	1.00020±0.00014
39	8	7	1.756	98.89	1.00062±0.00020
40	8	7	1.756	123.99	1.00011±0.00014
41	8	4	1.677	76.08	1.00020±0.00014
42	8	4	1.677	78.94	1.00042±0.00014
43	10	4	1.677	100.59	1.00042±0.00013
44	8	7	1.339	93.62	1.00024±0.00013
45	8	7	1.339	95.79	0.99998±0.00014
46	8	7	1.339	114.18	0.99969±0.00014
47	8	7	0.847	99.62	0.99935±0.00014
48	8	7	0.847	104.86	0.99974±0.00014
49	8	7	0.847	120.05	0.99887±0.00014
50	8	4	0.791	90.55	0.99917±0.00013
51	8	4	0.791	92.99	0.99911±0.00014
52	10	4	0.791	113.15	0.99983±0.00014
Avg.					**0.99974**

The results from Table 1 indicate excellent performance of the ENDF/B-VII nuclear cross-section data over the range of experimental variables. Due to the relatively narrow range of water-to-fuel ratios for the experiments, no immediately observable independent correlation variable could found to trend the data. Instead, the entire group of fifty-two data points will be treated as a single population sample. Statistical analyses of the data are presented in Figure 3.

Figure 3: Statistical Analysis of Eigenvalue Results.

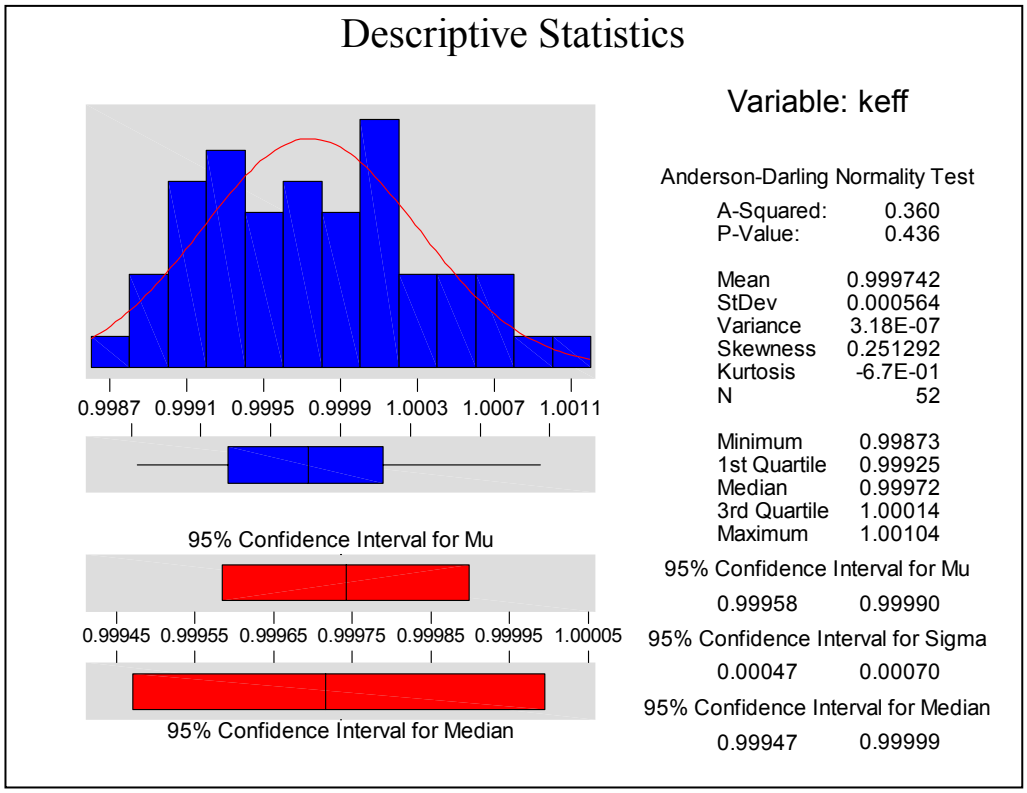

The results in Figure 3 indicate that the population sample is normally distributed about the mean and a 95% confidence interval for the mean (μ) ranging from 0.99958 to 0.99990. This represents an extremely small statistical spread in the data with a bias from 1.0 that is well within the reported measurement and statistical uncertainties of the experiments.

3 Fission Density Benchmark Comparison

In addition to integral critical configurations for a variety of UO_2 lattice configurations, individual, post-experiment, gross axial and radial gamma scans were performed on individual pins in tests #1 and #4. These measurements were taken to obtain relative pin-power fission density estimates for direct benchmark comparison to transport method calculations. Figures 4, 5 and 6 show some of the results. The MCNPX calculated individual pin fission density estimates for rods A, B and C show excellent agreement with the measured gross gamma scan results from the post-experiment exams. RMS errors are in the range from 1.4% to 1.7%. Even the minor effects of the thin (5mm) aluminum spacer that was inserted into the test zone region for these measurements (to ensure no pin movement) can be seen in the axial fission density plots for rods A and B. Almost no perturbation of the shape is seen in the rod that was outside the test zone (rod C).

Figure 4. Measured vs. Calculated Fission Densities - Rod A

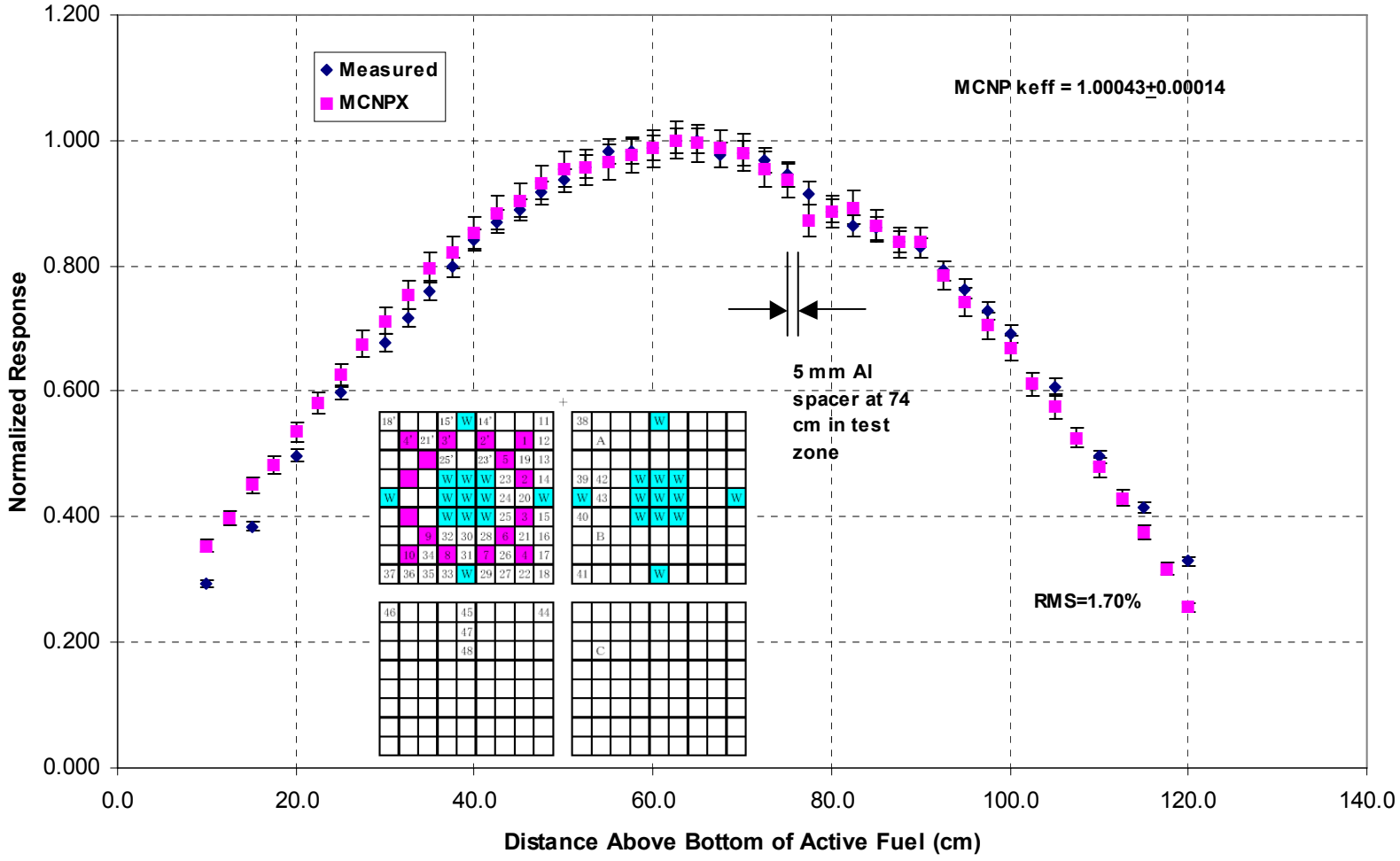

Figure 5. Measured vs. Calculated Fission Densities - Rod B

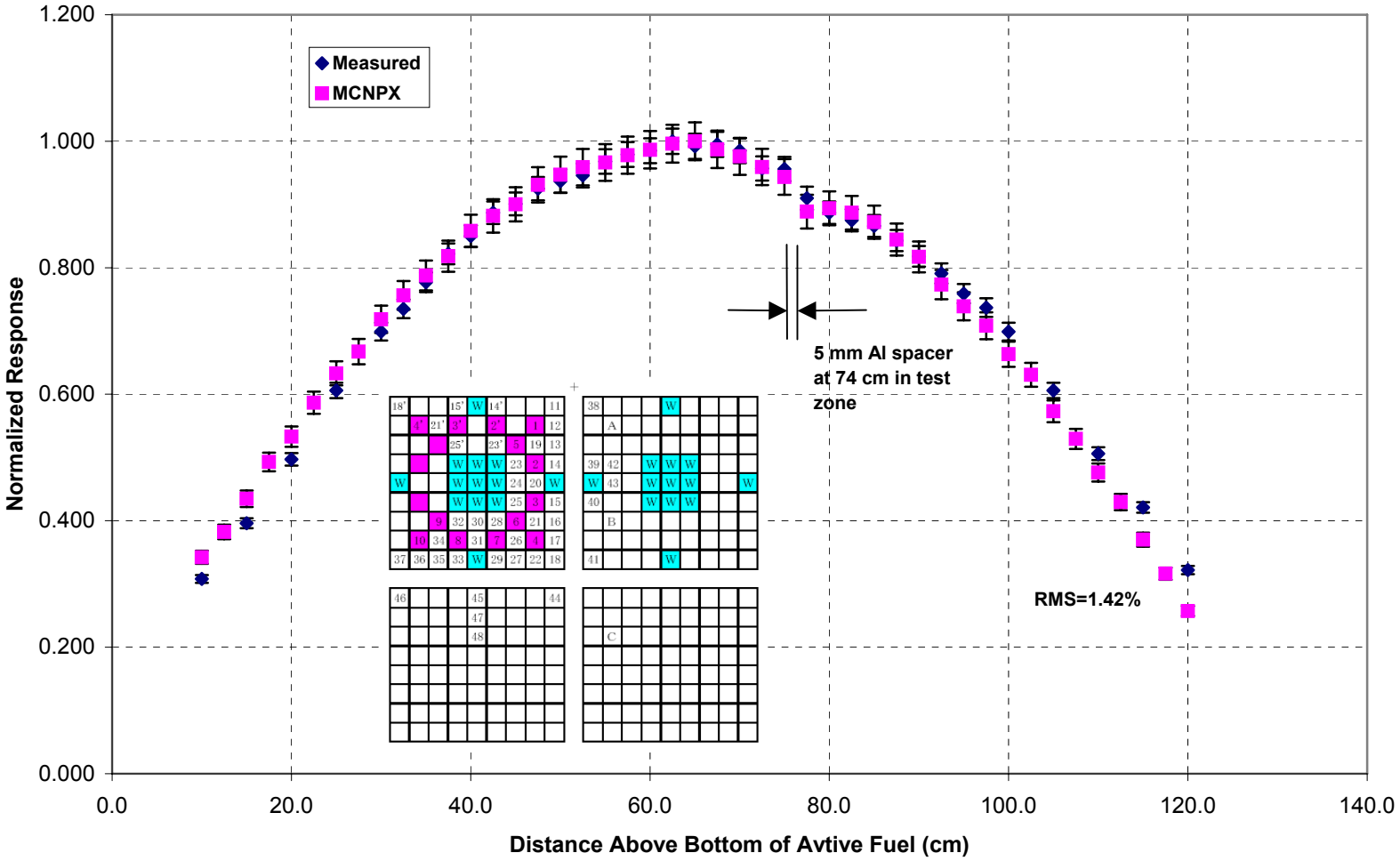

Figure 6. Measured vs. Calculated Fission Densities - Rod C

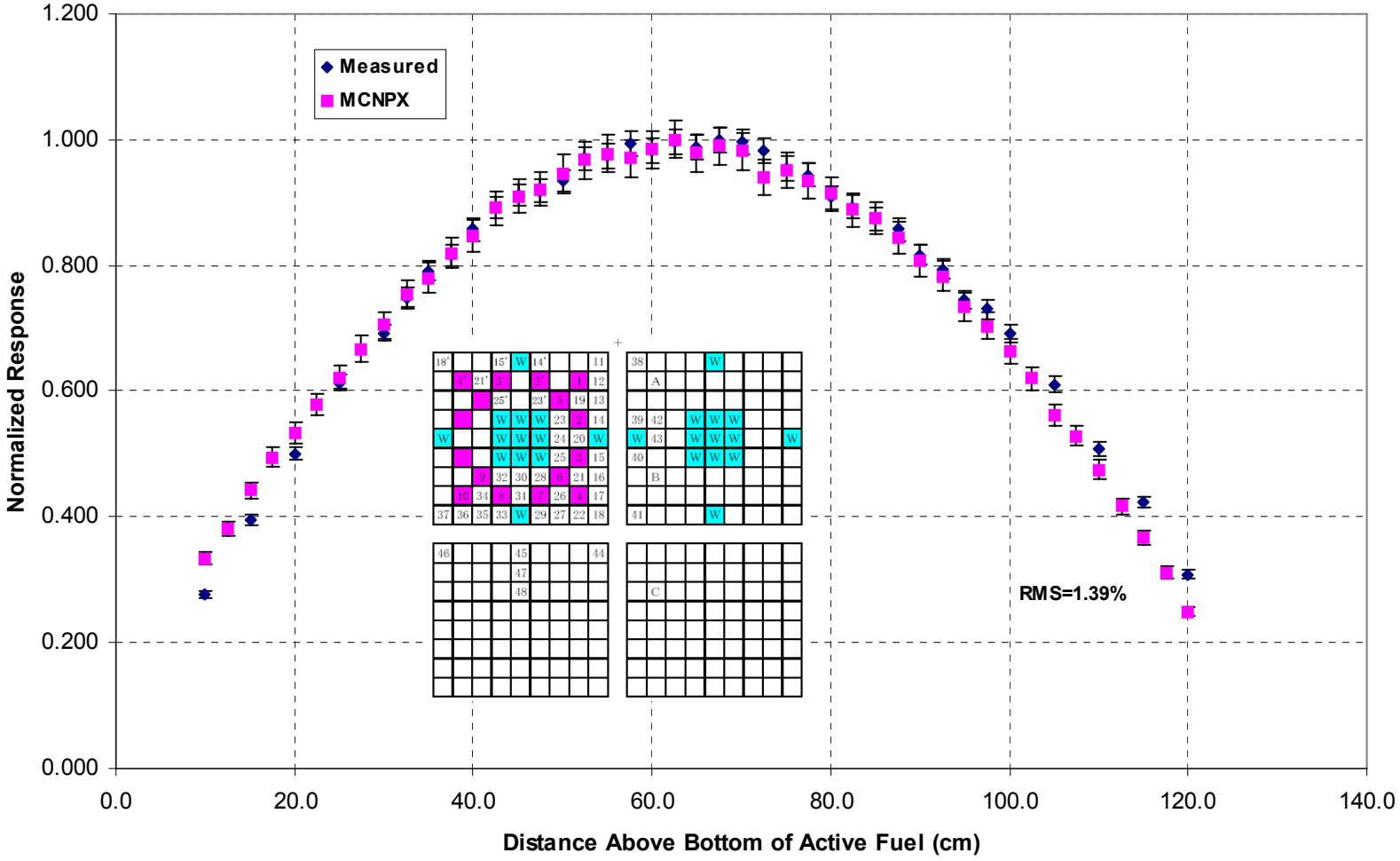

The final fission density comparisons will be made for 2-D radial measurements across the axial mid-plane of fuel bundles inside the test zone of experiments #1 and #4. For these tests, the selected individual fuel rods were removed and scanned over small section of the fuel rod near the core mid-plane. The gross gamma scan measurements were then tabulated and normalized to provide a 2-D pin power fission density distribution across the bundle/lattice. These results were then compared to direct Monte Carlo estimates at the same locations shown in Figures 7 and 8.

Figure 7: Percent Difference Between Measured and Calculated Fission Densities (case #1).

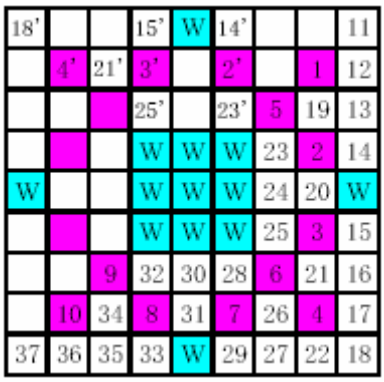

-2.726	0.063	0.980	**-1.075**	W	**-0.392**	-0.306	1.193	**-3.071**
1.738	**-2.043**	**0.386**	**-2.989**	1.957	**-2.041**	1.413	**-2.328**	**1.193**
0.018	1.946	-1.028	**-1.754**	-1.018	**-4.337**	**-3.724**	**1.413**	**-0.306**
-0.248	-1.995	-1.546	W	W	W	**-2.022**	**-1.400**	**-0.901**
W	1.572	-1.177	W	W	W	**-1.018**	**1.957**	W
1.101	-0.087	-1.111	W	W	W	**0.094**	**-1.621**	**-1.423**
0.063	1.516	**-1.059**	**-1.111**	**-1.177**	**-1.546**	**-1.028**	**0.170**	**0.980**
1.776	**-0.592**	**1.516**	**-0.087**	**1.572**	**-1.995**	**1.946**	**-0.676**	**0.063**
-0.540	**1.776**	**0.063**	**1.101**	W	**-0.248**	**0.018**	**1.738**	**-0.893**

RMS=2.20%

The values in bold represent the % difference between the measured data and the MCNPX calculated results. The remaining (non-bold) data points are the % differences based on inferred results assuming diagonal symmetry within the lattice. The purple values represent UO_2-Gad rods and the 'W' represents water rod locations. The total overall RMS difference between measured and calculated values is 2.20% for case #1 and 1.55% for case #4.

Figure 8: Percent Difference Between Measured and Calculated Fission Densities (case #4).

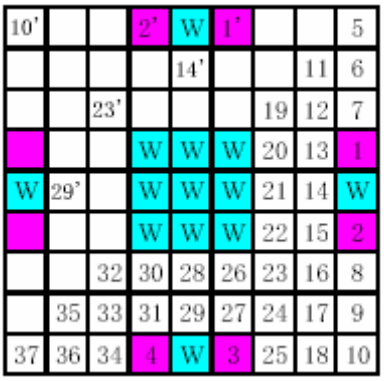

-0.324	0.783	1.162	**-1.242**	W	**-1.796**	0.137	-2.238	**-1.493**
2.927	1.853	0.218	-2.313	**1.840**	-1.828	3.012	**0.082**	**-2.238**
1.578	0.883	**2.759**	-1.609	-0.628	-3.716	**-2.723**	**3.012**	**0.137**
-2.143	1.181	0.119	W	W	W	**-3.716**	**-1.828**	**-2.410**
W	**0.606**	-0.575	W	W	W	**-0.628**	**-1.493**	W
-2.985	-0.622	-0.621	W	W	W	**-1.609**	**-2.313**	**-0.617**
-0.508	-1.118	**0.486**	**-0.621**	**-0.575**	**0.119**	**2.539**	**0.218**	**1.162**
-0.497	**2.045**	**-1.118**	**-0.622**	**0.592**	**1.181**	**0.883**	**1.853**	**0.783**
-0.968	**-0.497**	**0.521**	**-2.985**	W	**-2.143**	**1.578**	**2.927**	**0.380**

RMS=1.55%

4 Conclusions

The results of this benchmarking study are part of the validation basis for the use of MCNPX with ENDF/B-VII nuclear cross-section data for predicting the lattice physics behavior of low-enriched UO_2 pin lattice in water systems in the (W/F) range applicable to BWR fuel bundles. These 52 benchmark experiments are similar to those included in the International Handbook of Evaluated Criticality Safety Benchmark Experiments [5] for Low-Enriched Composite Thermal (LEU-COMP-THERM) systems with the notable exception that these experiments all contain gadolinium in the fuel as a burnable absorber. This feature, along with the presence of the hollow aluminum void tubes in the test zone lattices, makes them uniquely applicable to BWR fuel. Finally, the direct comparison of Monte Carlo results with those of estimated pin-power fission densities inside several of the test zone case bundle/lattices also serves to validate the use of MCNPX with ENDF/B-VII cross-sections for this application.

References

1) SCO-01-2047, “2001 Critical Examination of PLR/Corner Gad”, Toshiba Electric Power Corporation, December 2001.
2) NEDC-32906P, “MCNP:TGBLA03T/DIF3D:TGBLA06V/DIF3D Benchmarking of Toshiba’s NCA Critical Facility”, GE Nuclear Energy & Toshiba Corporation, May 1996
3) MCNPX, Version 2.6A, Los Alamos National Laboratory, LA-UR-05-8225, October 24, 2005
4) Knott, D, Wehlage, E., Zino, J. “A Comparison of Results from LANCER02 and MCNP on a Series of Two-Dimensional Multiple BWR Bundle Configurations”, American Nuclear Society’s Topical Meeting on Reactor Physics, PHYSOR 2006.
5) Nuclear Energy Agency, International Handbook of Evaluated Criticality Safety Benchmark Experiments, NEA/NSC/DOC (95) 03, September 2005 Edition